Thermal analysis model correction method based on Latin hypercube sampling and coordinate rotation method

Shijun Li, Liheng Chen & Shuai Liu

Published online: 10 Jul 2023.

Submit your article to this journal

Article views: 52

View related articles

View Crossmark data

Taylor & Francis
Taylor & Francis Group

Check for updates

Thermal analysis model correction method based on Latin hypercube sampling and coordinate rotation method

Shijun Li[a,b], Liheng Chen[a,c], and Shuai Liu[a,c]

[a]Changchun Institute of Optics, Fine Mechanics and Physics, Chinese Academy of Sciences, Changchun, Jilin, China; [b]Technology Development Limited Company of Beijing Nine Days Microsatellite, Beijing, China; [c]University of Chinese Academy of Sciences, Beijing, China

ABSTRACT

To predict on-orbit temperatures of the spacecraft accurately, a correction method for the thermal analysis model is proposed that combines Latin hypercube sampling and the coordinate rotation method. First, the thermal design parameters to be corrected are determined. Second, the thermal design parameters are sampled by the Latin hypercube sampling, and the sampling results inputted to the I-deas/TMG software for the thermal simulation calculation. Then according to the results of thermal simulation, the thermal design parameters are classified using the Spearman rank correlation coefficient formula, as either global sensitive parameters, local sensitive parameters, or insensitive parameters. Finally, according to the layered correction idea, the above parameters are corrected by the coordinate rotation method to find the optimal solution that satisfies the objective function. After the correction, the maximum temperature difference between the thermal simulation and the thermal balance test for each temperature measurement point is less than 1 °C for high-temperature conditions, and a maximum temperature difference of less than 2 °C for low-temperature condition.

1. Introduction

Spacecraft are very complex systems. When building a thermal analysis model, a large number of simplifying assumptions must be made, which inevitably introduce errors in the model [1]. To predict the on-orbit temperature of a spacecraft accurately, the thermal analysis model must be corrected based on temperature data of a thermal balance test [2]. With the increase in equipment on board spacecraft, more parameters need to be introduced into the thermal analysis model. The traditional "semi-experience-trial-method" and "least squares method" are inefficient and cannot be synchronized with the emerging computing software platforms [3].

In the early twenty first century, with the comprehensive development of computer technology, the parameter correction technique based on the Monte Carlo method for a spacecraft thermal network model has become, on the international level, a research hotspot in the field of space thermal analysis. In recent years, although the Monte Carlo method has achieved remarkable results in the application of the spacecraft thermal analysis model correction, exceeding those of traditional methods [4], its effect when used alone is also very general [5].

Previous studies have shown that, if the thermal design parameters are corrected directly, there are often many peaks of the inversion error surface. All the correction parameters are unable to reach their optimal values at the same time [6]. Therefore, the temperature field should first be classified according to the

sensitivity of the thermal design parameters. According to the classified results, the thermal design parameters are gradually corrected by the layered correction idea [7], that is, the primary influence parameters are initially corrected, then the secondary influence parameters are corrected, and finally those with almost no influence are left untouched. To further improve the correction accuracy, an in-depth study based on the Monte Carlo method is performed, and a thermal analysis model correction method combining Latin hypercube sampling (LHS) and the coordinate rotation method (CRM) is introduced. At the same time, the idea of a layered correction is implemented during the correction.

Taking the solar X-ray and extreme ultraviolet imager (XEUVI) as an example, and using the temperature data of the thermal balance test at high-temperature condition, LHS, the CRM, and the layered correction idea are applied to complete the calculation for thermal analysis model correction, and the low-temperature condition is used to verify the result.

2. Thermal balance test

The XEUVI is designed to operate in a sun-synchronous orbit with a track height of 836 km and an orbit inclination of 98.76°; the local time of the satellite through the ascending node is 5:40 am. The XEUVI's forward flight direction is defined as the $+X$ direction, whereas the direction toward the ground is defined as the $+Z$ direction; the right-hand rule determines the $+Y$ direction.

2.1. Test scheme

In the thermal balance test for the XEUVI, the space environment is simulated using a space environment simulator and the absorbed external heat fluxes are simulated using heaters [8, 9]. Heaters attached to the outer surfaces simulate the external heat fluxes absorbed by the MLI surfaces. The external heat fluxes absorbed by the light entrances (including the entrances of the primary optical tube, guide telescope, and photometer) are simulated using a heater attached to the surface of each. In addition, the satellite platform is configured as a10 mm-thick aluminum plate, the temperature of which is controlled by attaching heaters to its surface and simultaneously insulating it from the pedestal (Figure 1).

2.2. Thermal balance test conditions

Two extreme conditions were simulated by varying the external heat fluxes, working mode, distribution of internal heat sources, and thermal properties of the thermal control layer. The specific settings are listed in Table 1.
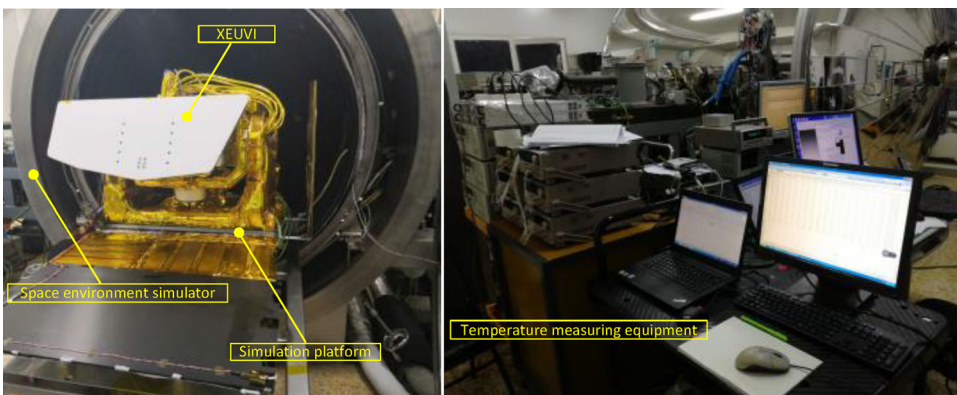

Figure 1. Physical layout of the thermal balance test.

Table 1. Thermal balance test conditions.

No.	Condition label	Main setting conditions
1	Low temperature	The β-angle is 88.6°, the solar constant is 1414 W/m², and the pointing mechanism is rotated according to the solar vector on October 16. The performance parameter of the F46 membrane is $\alpha s/\varepsilon = 0.15/0.69$, and the performance parameter of the S781 white paint is $\alpha s/\varepsilon = 0.17/0.86$. Both the internal heat source and the active thermal control are operating, and the temperature of simulated platform is $-20\,°C$.
2	High temperature	The β-angle is 88.6°, the solar constant is 1414 W/m², and the pointing mechanism is rotated according to the solar vector on October 16. The performance parameter of the F46 membrane is $\alpha s/\varepsilon = 0.36/0.69$, and the performance parameter of the S781 white paint is $\alpha s/\varepsilon = 0.40/0.86$. The internal heat source works and the active thermal control works, and the temperature of simulated platform is $45\,°C$.

2.3. Test results and analysis

According to the designed conditions, the thermal balance test was performed first at the low temperature and then at the high temperature. The degree of vacuum during the thermal balance test was 5×10^{-5} Pa, and the heat sink temperature was 100 K. The test results are given as temperature curves (Figures 2 and 3) of the key components of the XEUVI under different conditions.

At the same time, from the test results, the temperature data of the temperature measurement points (TMPs) of the XEUVI under various conditions were also collected, including that of the CCD, motor, and electric box. From the position, code, temperature, and thermal control index (TCI) of the TMPs (Table 2), we see that the CCD temperature is $-65.35\,°C$, the motor temperature ranges from $8.90\,°C$ to $10.45\,°C$, and the electrical box temperature ranges from $4.15\,°C$ to $29.00\,°C$; all three satisfy the TCI. The remaining components also meet the TCI. The thermal balance test verified the correctness of the thermal design and provided a basis for thermal analysis model corrections.

3. Thermal analysis model

According to the state of the test piece during the thermal balance test, a finite element model for thermal analysis was established with I-deas/TMG software (Figure 4). The thin-walled components in the XEUV imager are simplified through use of shell elements, and the thicknesses of these elements are calculated based on the volume equivalent thickness. The model is divided into 9995 elements. During modeling, the thermal coupling method is used to simplify the process. A total of 178 thermal couplings were established within the thermal analysis model. The optical components are modeled with solid elements. In addition, the boundary conditions, the internal heat source, the location of the TMP, and the applied external heat fluxes of the thermal analysis model are also consistent with the test state.

4. Thermal analysis model correction

4.1. Process of thermal analysis model correction

For the thermal analysis model correction (Figure 5), key thermal design parameters are as much as possible selected first. The thermal design parameters are sampled next using LHS; the sampling results are then inputted to the I-deas/TMG software for thermal simulation calculations. Next, depending on the results of the thermal simulation, the thermal design parameters are classified as either global sensitive parameters, local sensitive parameters or insensitive parameters using the Spearman rank correlation coefficient formula. Global-sensitive and local-sensitive parameters are mainly corrected, whereas those parameters with almost no influence are left untouched. Finally, according to this layered correction idea, the CRM is used to correct the global and local sensitive parameters, and combinations of them are constantly iterated until the iterative error of the objective function is satisfied and an optimal solution obtains.
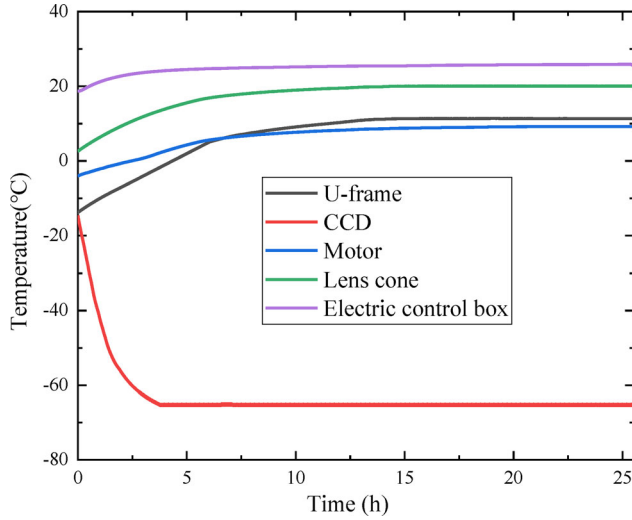
Figure 2. Temperature curve of key components at low temperature condition.
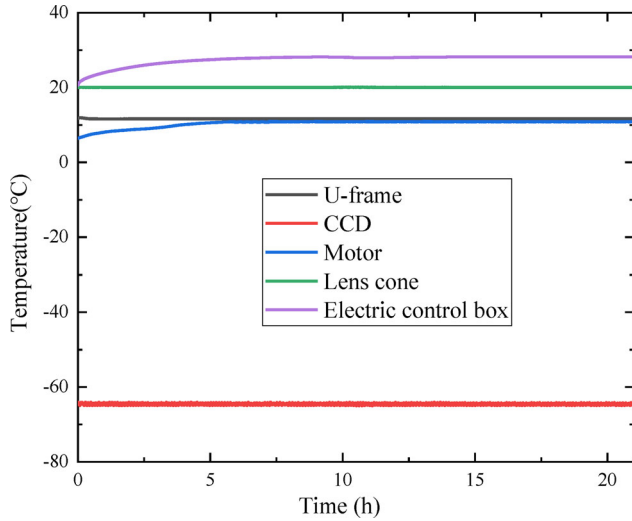

Figure 3. Temperature curve of key components at high temperature condition.

4.2. Objective function

Parameter corrections of the spacecraft thermal analysis model are the result of a known problem. The inverse solution is the process of finding the input parameter variables [10]. In general, the input–output relationship of the spacecraft thermal analysis model can be described by geometric models and the thermal mathematical model, respectively, but introduces numerous geometric parameters and thermophysical parameters. The input–output relationship is expressed as a multidimensional complex function,

$$\vec{T} = F(\vec{X}), \tag{1}$$

where $\vec{T}$ is the output temperature vector of the n-dimensional model, $\vec{X}$ the input parameter vector of the m-dimensional model, and F is the $n \times m$-order solution operator from $\vec{X}$ to $\vec{T}$.

Table 2. Temperature of key components (units: °C).

No.	Name	TMP	High temperature	Low temperature	TCI
1	CCD	T_1	−65.35	−65.35	−70∼−55
2	Thermal strap (−Y)	T_2	−65.81	−65.92	−90∼−50
3	Thermal strap (+Y)	T_3	−71.55	−72.76	−90∼−50
4	Radiant plate	T_4	−75.55	−76.95	−100∼−50
5	Box (+Y)	T_5	−12.10	−15.29	−25∼30
6	Box (−X)	T_6	−8.25	−11.77	−25∼30
7	Light entrance	T_7	48.85	31.01	−15∼60
8	Lens cone	T_8	20.60	18.70	10∼30
9	Guide telescope	T_9	17.35	15.25	10∼30
10	Electric box of guide telescope	T_{10}	16.75	14.95	10∼30
11	U-frame (+X)	T_{11}	10.45	9.95	−5∼25
12	U-frame (−X)	T_{12}	10.45	9.40	−5∼25
13	O-frame (−Z)	T_{13}	8.90	6.75	0∼30
14	O-frame (+Z)	T_{14}	13.65	10.45	0∼30
15	Motor 1	T_{15}	10.45	9.95	0∼45
16	Motor 2	T_{16}	9.95	8.90	0∼45
17	Encoder	T_{17}	−4.90	−6.56	−15∼45
18	Control electric box	T_{18}	29.00	25.70	−15∼45
19	Boost electric box	T_{19}	4.80	8.15	−15∼45
20	Piezoelectric drive electric box	T_{20}	7.85	4.15	−15∼45

Introducing the test temperature vector $\vec{T}_0$, and error vector $\vec{e} = \vec{T} - \vec{T}_0$, the problem addressed in model correction reduces to finding a certain norm minimum value for $\vec{e}$, that is,

$$\text{Object} = \min \ \|\vec{e}\|. \tag{2}$$

The main research purpose of thermal analysis model correction theory of spacecraft is to find an effective engineering method, ensuring the inversion parameter vector satisfies condition (2).

4.3. Selection of thermal design parameter

The thermal design parameters of spacecraft are important influencing factors in thermal analysis calculations, and are also the main content of thermal analysis model corrections. The thermal design parameters mainly include contact thermal resistance, thermal conductivity of material, coefficient of radiation heat transfer between multilayer and load, and emissivity of the coating, all of which need to be considered. According to the above thermal design principles, the thermal design parameters of the XEUVI are sorted out, and a total of 50 thermal design parameters are selected, including contact thermal resistances (37), coefficients of radiation heat transfer between components and multiple layers (11), surface emissivity of the aluminum film (1), and thermal conductivity of the copper thermal strap (1). The name, code, location, and range of value of each parameter are listed in Table 3.

4.4. Latin hypercube sampling

LHS is an effective uniform sampling with high sample coverage that avoids a large number of repeated samplings [11–14]. The basic idea of this sampling is to divide each random parameter $x_i \in X$ into equal parts according to the probability size N in the distribution space. The calculation strictly guarantees that it is sampled once in each aliquot [15].

To understand the effect of the LHS method more intuitively, 400 samplings of four different thermal design parameters were taken. The results of the sampling are displayed as a frequency distribution histogram (Figure 6). The sampling frequency fluctuation of each interval is small, indicating that each individual input is covered uniformly.
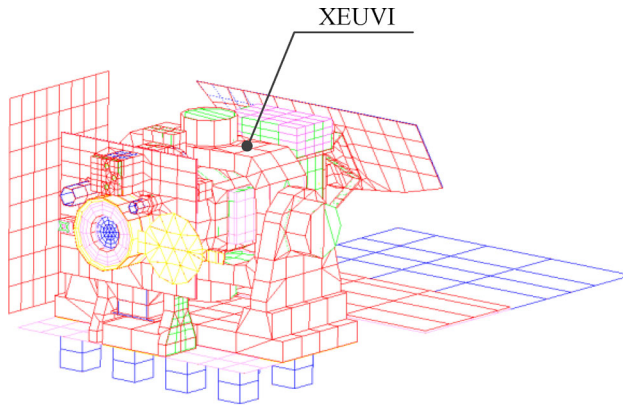
Figure 4. Thermal analysis model of the XEUVI.

4.5. Sensitivity classification of thermal design parameters

To study the sensitivity of each TMP relative to the selected thermal design parameters, a Spearman rank correlation coefficient is introduced that is calculated as follows [16]:

$$R_s = 1 - \frac{6 \sum_{i=1}^{N} [O(Ci) - O(Ti)]^2}{N(N^2 - 1)} \tag{3}$$

where N is the number of samplings, Ci the sampling value of the thermal design parameters, Ti the temperature of the TMP, and $O(X)$ the sequence number of its argument $X = C_i$, T_i when the N sampling parameters are sorted in ascending or descending order.

If the Spearman rank correlation coefficient R_S of a parameter for the temperature of all TMPs satisfies $Rs \geq 0.3$, the parameter is called a global sensitive parameter. If R_S of a parameter for the temperature of only a subset of all TMPs satisfies $Rs \geq 0.3$, the parameter is called a local sensitive parameter. If R_S of a parameter to the temperature of all TMPs does not satisfied $Rs \geq 0.3$, the parameter is called an insensitive parameter.

The 50 thermal design parameters are sampled 400 times using the LHS, and the results of the sampling are inputted to the I-deas/TMG software for calculation. Then, the MATLAB program is used to calculate R_S of the 50 thermal design parameters with respect to 20 TMPs.

In order to reveal the correlations, (a) among inputs, (b) among the 20 output variables, and (c) among inputs and outputs, a 70*70 matrix named E is given, which is split into 4 matrices, including A, B, B^T and C.

$$E = \begin{bmatrix} A & B \\ B^T & C \end{bmatrix}_{70 \times 70}$$

A matrix is a diagonal square block 50×50 for the correlation in the 400 LHS-sampled values for the 50 input variables (C1~C50). The correlation in the 400 LHS-sampled values for the 50 input variables is summarized, and presenting graphically the correlations among inputs in a form of small colored matrix without numbers, where the color will show the correlations (three colors showing the absolute values in ranges 0-0.3 (dark blue), 0.3-0.7 (green) and 0.7-1.0 (yellow)).
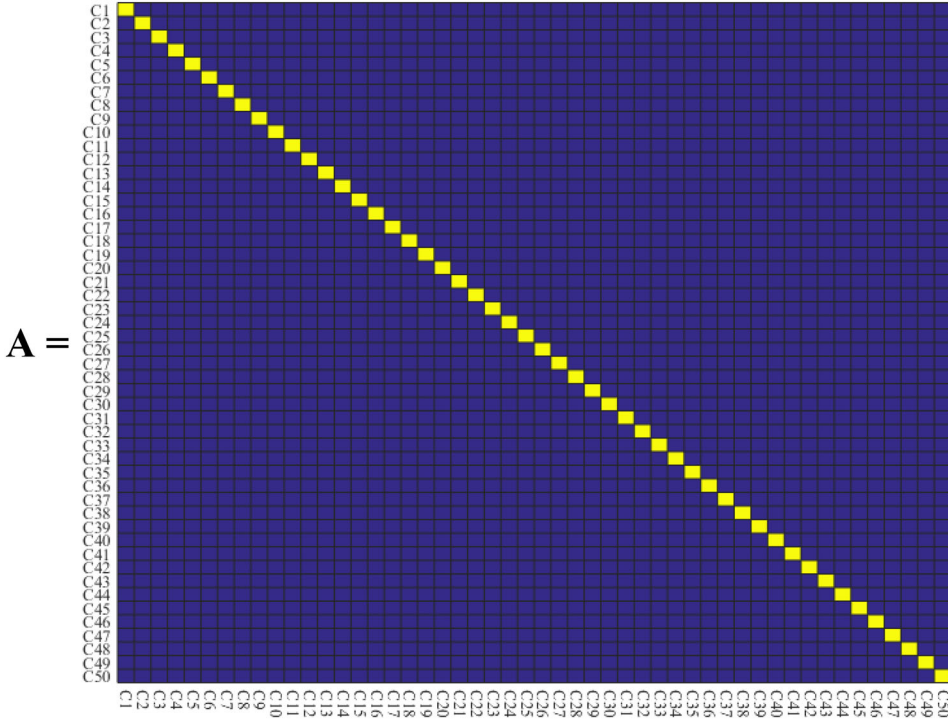
C matrix is a diagonal square block 20×20 for the output variables (T1~T20).

$$C = \begin{bmatrix} T1 & & & & \\ & T2 & & & \\ & & \ddots & & \\ & & & T20 \end{bmatrix}_{20 \times 20}$$

B matrix is a block 50×20 that the MATLAB program is used to calculate RS of the 50 thermal design parameters with respect to 20 TMPs. BT represents the transposed matrix of B.

$$
B = \begin{bmatrix}
0.06 & 0.02 & 0.08 & 0.04 & 0.05 & 0.02 & 0.07 & 0.01 & 0.06 & 0.11 & 0.08 & 0.01 & 0.03 & 0.09 & 0.06 & 0.13 & 0.02 & 0.07 & 0.02 & 0.07 \\
0.01 & 0.08 & 0.00 & 0.04 & 0.03 & 0.01 & 0.10 & 0.03 & 0.02 & 0.03 & 0.11 & 0.05 & 0.04 & 0.18 & 0.09 & 0.10 & 0.04 & 0.01 & 0.02 & 0.10 \\
0.01 & 0.04 & 0.09 & 0.07 & 0.07 & 0.04 & 0.05 & 0.01 & 0.09 & 0.14 & 0.11 & 0.10 & 0.08 & 0.03 & 0.08 & 0.14 & 0.03 & 0.06 & 0.14 & 0.01 \\
0.05 & 0.07 & 0.09 & 0.15 & 0.07 & 0.00 & 0.10 & 0.02 & 0.01 & 0.20 & 0.05 & 0.02 & 0.13 & 0.11 & 0.07 & 0.01 & 0.00 & 0.13 & 0.08 & 0.05 \\
0.06 & 0.02 & 0.06 & 0.05 & 0.10 & 0.08 & 0.07 & 0.04 & 0.05 & 0.01 & 0.17 & 0.11 & 0.07 & 0.03 & 0.04 & 0.00 & 0.03 & 0.09 & 0.04 & 0.02 \\
0.05 & 0.08 & 0.01 & 0.05 & 0.08 & 0.06 & 0.19 & 0.08 & 0.03 & 0.03 & 0.04 & 0.05 & 0.10 & 0.05 & 0.07 & 0.04 & 0.02 & 0.02 & 0.06 & 0.16 \\
0.09 & 0.05 & 0.03 & 0.03 & 0.12 & 0.19 & 0.03 & 0.02 & 0.11 & 0.04 & 0.03 & 0.04 & 0.03 & 0.07 & 0.12 & 0.06 & 0.11 & 0.00 & 0.03 & 0.01 \\
0.01 & 0.08 & 0.19 & 0.06 & 0.08 & 0.05 & 0.18 & 0.07 & 0.10 & 0.08 & 0.07 & 0.04 & 0.24 & 0.02 & 0.06 & 0.11 & 0.02 & 0.06 & 0.01 & 0.10 \\
0.17 & 0.06 & 0.05 & 0.10 & 0.05 & 0.10 & 0.01 & 0.01 & 0.04 & 0.01 & 0.03 & 0.04 & 0.04 & 0.08 & 0.02 & 0.03 & 0.01 & 0.03 & 0.16 & 0.16 \\
0.14 & 0.06 & 0.08 & 0.01 & 0.05 & 0.19 & 0.05 & 0.01 & 0.02 & 0.01 & 0.13 & 0.01 & 0.00 & 0.03 & 0.00 & 0.14 & 0.00 & 0.01 & 0.02 & 0.18 \\
0.10 & 0.13 & 0.08 & 0.18 & 0.13 & 0.03 & 0.06 & 0.00 & 0.04 & 0.02 & 0.02 & 0.04 & 0.02 & 0.02 & 0.04 & 0.01 & 0.05 & 0.07 & 0.08 & 0.06 \\
0.01 & 0.01 & 0.05 & 0.01 & 0.02 & 0.09 & 0.04 & 0.13 & 0.09 & 0.00 & 0.14 & 0.06 & 0.09 & 0.02 & 0.05 & 0.07 & 0.06 & 0.04 & 0.08 & 0.05 \\
0.10 & 0.02 & 0.02 & 0.12 & 0.13 & 0.01 & 0.08 & 0.02 & 0.01 & 0.04 & 0.18 & 0.04 & 0.04 & 0.09 & 0.03 & 0.08 & 0.14 & 0.10 & 0.01 & 0.01 \\
0.10 & 0.21 & 0.13 & 0.19 & 0.04 & 0.01 & 0.03 & 0.09 & 0.01 & 0.17 & 0.04 & 0.02 & 0.03 & 0.05 & 0.06 & 0.06 & 0.00 & 0.00 & 0.04 & 0.04 \\
0.20 & 0.08 & 0.05 & 0.12 & 0.10 & 0.12 & 0.00 & 0.00 & 0.09 & 0.04 & 0.04 & 0.15 & 0.12 & 0.10 & 0.05 & 0.00 & 0.09 & 0.04 & 0.02 & 0.01 \\
0.06 & 0.05 & 0.08 & 0.04 & 0.09 & 0.08 & 0.04 & 0.00 & 0.07 & 0.21 & 0.08 & 0.02 & 0.04 & 0.03 & 0.06 & 0.07 & 0.01 & 0.01 & 0.05 & 0.04 \\
0.02 & 0.09 & 0.04 & 0.01 & 0.02 & 0.06 & 0.03 & 0.07 & 0.10 & 0.21 & 0.06 & 0.08 & 0.02 & 0.06 & 0.07 & 0.04 & 0.04 & 0.10 & 0.07 & 0.03 \\
0.06 & 0.04 & 0.07 & 0.04 & 0.05 & 0.00 & 0.04 & 0.04 & 0.01 & 0.06 & 0.03 & 0.06 & 0.03 & 0.01 & 0.14 & 0.05 & 0.14 & 0.01 & 0.02 & 0.02 \\
0.03 & 0.01 & 0.01 & 0.05 & 0.12 & 0.12 & 0.02 & 0.06 & 0.05 & 0.16 & 0.10 & 0.14 & 0.01 & 0.11 & 0.02 & 0.08 & 0.07 & 0.00 & 0.13 & 0.07 \\
0.02 & 0.06 & 0.11 & 0.03 & 0.17 & 0.12 & 0.09 & 0.03 & 0.01 & 0.08 & 0.01 & 0.03 & 0.05 & 0.00 & 0.00 & 0.02 & 0.07 & 0.01 & 0.03 & 0.03 \\
0.31 & 0.31 & 0.44 & 0.32 & 0.56 & 0.76 & 0.32 & 0.31 & 0.32 & 0.42 & 0.32 & 0.32 & 0.36 & 0.39 & 0.31 & 0.41 & 0.38 & 0.63 & 0.54 & 0.31 \\
0.16 & 0.22 & 0.16 & 0.06 & 0.10 & 0.07 & 0.09 & 0.04 & 0.07 & 0.14 & 0.02 & 0.01 & 0.01 & 0.07 & 0.03 & 0.06 & 0.05 & 0.04 & 0.17 & 0.18 \\
0.08 & 0.04 & 0.02 & 0.00 & 0.06 & 0.04 & 0.01 & 0.11 & 0.03 & 0.16 & 0.02 & 0.07 & 0.02 & 0.05 & 0.16 & 0.00 & 0.05 & 0.05 & 0.01 & 0.03 \\
0.01 & 0.33 & 0.33 & 0.16 & 0.00 & 0.03 & 0.00 & 0.30 & 0.01 & 0.01 & 0.57 & 0.39 & 0.10 & 0.00 & 0.42 & 0.01 & 0.02 & 0.46 & 0.31 & 0.05 \\
0.10 & 0.02 & 0.04 & 0.09 & 0.04 & 0.06 & 0.02 & 0.10 & 0.07 & 0.10 & 0.04 & 0.07 & 0.11 & 0.00 & 0.06 & 0.24 & 0.03 & 0.09 & 0.06 & 0.03 \\
0.03 & 0.03 & 0.18 & 0.06 & 0.06 & 0.06 & 0.42 & 0.07 & 0.06 & 0.52 & 0.09 & 0.04 & 0.22 & 0.32 & 0.05 & 0.36 & 0.76 & 0.04 & 0.06 & 0.10 \\
0.11 & 0.05 & 0.00 & 0.01 & 0.20 & 0.07 & 0.04 & 0.08 & 0.05 & 0.07 & 0.09 & 0.02 & 0.04 & 0.06 & 0.05 & 0.10 & 0.02 & 0.06 & 0.07 & 0.07 \\
0.45 & 0.30 & 0.04 & 0.15 & 0.02 & 0.06 & 0.38 & 0.05 & 0.60 & 0.39 & 0.07 & 0.08 & 0.18 & 0.01 & 0.03 & 0.08 & 0.43 & 0.01 & 0.50 & 0.03 \\
0.02 & 0.00 & 0.01 & 0.10 & 0.03 & 0.01 & 0.11 & 0.08 & 0.04 & 0.01 & 0.04 & 0.01 & 0.05 & 0.06 & 0.04 & 0.18 & 0.11 & 0.05 & 0.05 & 0.04 \\
0.18 & 0.12 & 0.04 & 0.02 & 0.24 & 0.07 & 0.06 & 0.05 & 0.03 & 0.07 & 0.01 & 0.04 & 0.02 & 0.08 & 0.08 & 0.08 & 0.03 & 0.02 & 0.04 & 0.02 \\
0.31 & 0.34 & 0.49 & 0.27 & 0.03 & 0.02 & 0.05 & 0.09 & 0.01 & 0.14 & 0.14 & 0.01 & 0.10 & 0.09 & 0.06 & 0.03 & 0.15 & 0.12 & 0.06 & 0.07 \\
0.03 & 0.05 & 0.04 & 0.04 & 0.04 & 0.03 & 0.01 & 0.09 & 0.08 & 0.08 & 0.01 & 0.25 & 0.07 & 0.11 & 0.55 & 0.12 & 0.11 & 0.12 & 0.09 & 0.01 \\
0.10 & 0.05 & 0.02 & 0.03 & 0.01 & 0.04 & 0.05 & 0.10 & 0.02 & 0.10 & 0.18 & 0.04 & 0.00 & 0.04 & 0.20 & 0.00 & 0.04 & 0.14 & 0.04 & 0.06 \\
0.01 & 0.07 & 0.03 & 0.02 & 0.09 & 0.06 & 0.05 & 0.10 & 0.04 & 0.05 & 0.15 & 0.00 & 0.02 & 0.01 & 0.00 & 0.03 & 0.08 & 0.03 & 0.06 & 0.13 \\
0.00 & 0.07 & 0.02 & 0.03 & 0.07 & 0.02 & 0.02 & 0.00 & 0.02 & 0.02 & 0.04 & 0.11 & 0.13 & 0.07 & 0.01 & 0.00 & 0.24 & 0.00 & 0.06 & 0.09 \\
0.04 & 0.03 & 0.07 & 0.04 & 0.04 & 0.06 & 0.02 & 0.06 & 0.02 & 0.01 & 0.02 & 0.07 & 0.06 & 0.08 & 0.00 & 0.15 & 0.01 & 0.03 & 0.05 & 0.04 \\
0.08 & 0.05 & 0.03 & 0.14 & 0.04 & 0.12 & 0.01 & 0.03 & 0.01 & 0.02 & 0.03 & 0.08 & 0.01 & 0.04 & 0.03 & 0.01 & 0.11 & 0.06 & 0.06 & 0.07 \\
0.14 & 0.04 & 0.30 & 0.09 & 0.33 & 0.08 & 0.01 & 0.02 & 0.16 & 0.07 & 0.51 & 0.67 & 0.03 & 0.30 & 0.32 & 0.06 & 0.01 & 0.39 & 0.34 & 0.35 \\
0.66 & 0.57 & 0.61 & 0.84 & 0.36 & 0.39 & 0.38 & 0.36 & 0.46 & 0.35 & 0.37 & 0.39 & 0.42 & 0.37 & 0.38 & 0.50 & 0.35 & 0.42 & 0.31 & 0.37 \\
0.36 & 0.34 & 0.33 & 0.37 & 0.63 & 0.63 & 0.35 & 0.38 & 0.49 & 0.54 & 0.36 & 0.33 & 0.37 & 0.33 & 0.35 & 0.31 & 0.46 & 0.67 & 0.49 & 0.55 \\
0.08 & 0.08 & 0.04 & 0.37 & 0.04 & 0.12 & 0.01 & 0.03 & 0.43 & 0.07 & 0.22 & 0.02 & 0.93 & 0.07 & 0.13 & 0.34 & 0.39 & 0.04 & 0.48 & 0.41 \\
0.04 & 0.00 & 0.04 & 0.08 & 0.10 & 0.04 & 0.02 & 0.02 & 0.09 & 0.15 & 0.06 & 0.07 & 0.07 & 0.62 & 0.03 & 0.16 & 0.06 & 0.03 & 0.21 & 0.38 \\
0.45 & 0.09 & 0.33 & 0.34 & 0.04 & 0.03 & 0.12 & 0.02 & 0.31 & 0.03 & 0.05 & 0.16 & 0.04 & 0.01 & 0.05 & 0.11 & 0.00 & 0.37 & 0.47 & 0.39 \\
0.12 & 0.01 & 0.01 & 0.38 & 0.14 & 0.46 & 0.06 & 0.01 & 0.24 & 0.69 & 0.10 & 0.11 & 0.02 & 0.03 & 0.02 & 0.36 & 0.03 & 0.00 & 0.09 & 0.06 \\
0.13 & 0.10 & 0.00 & 0.10 & 0.01 & 0.04 & 0.03 & 0.00 & 0.04 & 0.09 & 0.11 & 0.02 & 0.09 & 0.02 & 0.08 & 0.19 & 0.00 & 0.09 & 0.10 & 0.10 \\
0.02 & 0.06 & 0.32 & 0.48 & 0.32 & 0.19 & 0.03 & 0.53 & 0.06 & 0.40 & 0.07 & 0.32 & 0.03 & 0.00 & 0.18 & 0.05 & 0.08 & 0.34 & 0.30 & 0.04 \\
0.04 & 0.06 & 0.00 & 0.09 & 0.11 & 0.08 & 0.07 & 0.02 & 0.02 & 0.03 & 0.11 & 0.10 & 0.03 & 0.02 & 0.05 & 0.03 & 0.06 & 0.02 & 0.11 & 0.12 \\
0.46 & 0.37 & 0.37 & 0.38 & 0.34 & 0.35 & 0.51 & 0.32 & 0.32 & 0.30 & 0.35 & 0.37 & 0.56 & 0.56 & 0.33 & 0.45 & 0.50 & 0.35 & 0.36 & 0.59 \\
0.37 & 0.37 & 0.48 & 0.52 & 0.08 & 0.44 & 0.01 & 0.05 & 0.37 & 0.07 & 0.11 & 0.03 & 0.30 & 0.01 & 0.22 & 0.02 & 0.41 & 0.03 & 0.54 & 0.35 \\
0.02 & 0.03 & 0.03 & 0.05 & 0.02 & 0.06 & 0.07 & 0.11 & 0.06 & 0.01 & 0.16 & 0.06 & 0.10 & 0.02 & 0.03 & 0.06 & 0.14 & 0.01 & 0.00 & 0.03
\end{bmatrix}_{50 \times 20}
$$

The classification results have been marked in the B matrix, where red marks represent global sensitive parameters (C21, C39, C40, C48), magenta marks represent local sensitive parameters (C24, C26, C28, C31, C32, C38, C41, C42, C43, C44, C46, C49), and unmarked ones are insensitive parameters.

4.6. Coordinate rotation method

The coordinate rotation method is also called "variable rotation method," "alternating method" or "dimension reduction method" [17, 18]. The basic idea is that, by "one time only one variable in the multivariate function is explored along its coordinate axis for one-dimensional exploration, the other variables are fixed, and the coordinate axes of one-dimensional exploration are sequentially rotated to complete the first round of exploration. Then going back to the second round of exploration until the objective function is found at the minimum point of the whole domain, in order to achieve the purpose of transforming a multidimensional unconstrained optimization
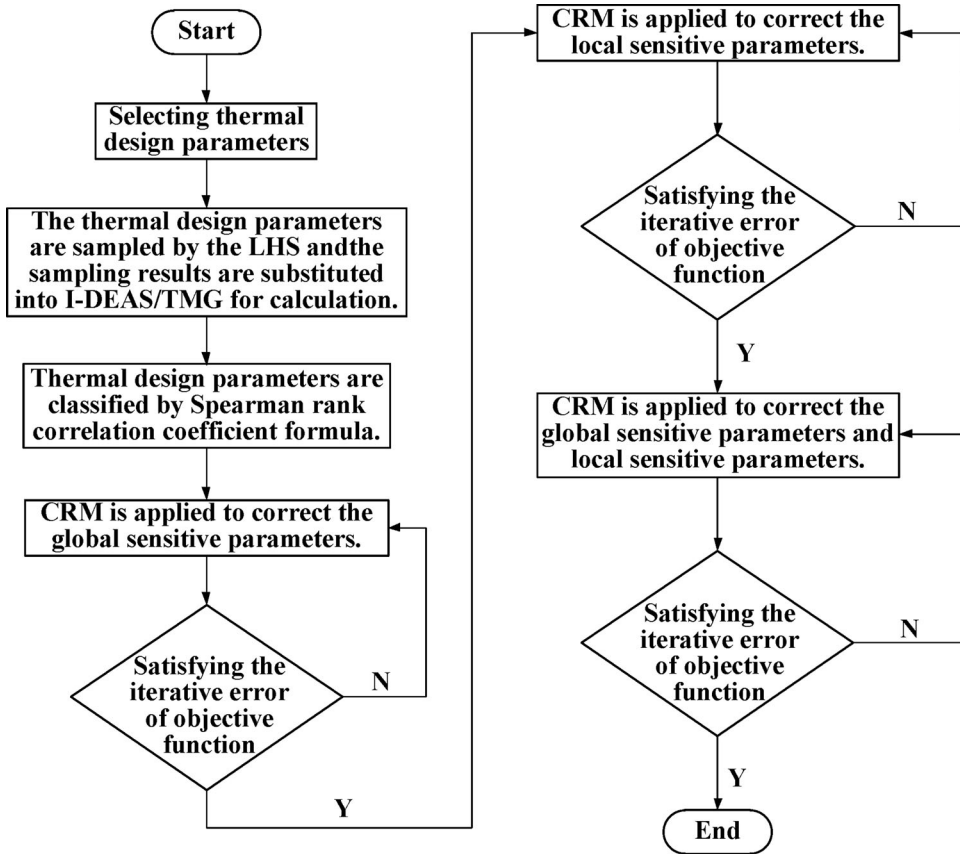
Figure 5. Process of thermal analysis model correction.

problem into a one-dimensional problem of some columns." The method does not need to determine the analytical formula of the objective function, nor does it need to solve the reciprocal of the objective function. The method is simple and easy to understand.

4.7. Correction method

First, during corrections, the optimal solution of the 400 different LHSs is taken as the initial value. Second, the CRM is applied to the four global sensitive parameters to determine the first round of corrections [19]. Then, taking these results of the first round as the initial value, the CRM is applied to the twelve local sensitive parameters to generate the second round of corrections. Finally, the CRM is applied to the four global sensitive parameters simultaneously and twelve local sensitive parameters to provide a third round of corrections, taking the correction result of the second round as the initial value. The correction result of the third round is the global optimal solution.

Figure 7 shows the objective function value of pre-corrections of the thermal model, the optimal solution of 400 different LHSs, and the results of each subsequent correction. The objective function value finally converges to 2.15. From Figure 7, the objective function values of the 400 different LHSs and the first-round corrections for the global sensitive parameters decrease the fastest.

Table 3. Statistics of thermal design parameters.

Name	Position	Code	Range
Thermal resistance (°C/W)	Between U-frame and Pedestal	C_1	0.4~2
	Between O-frame and Motor	C_2	10~40
	Between U-frame and Encoder	C_3	0.5~3
	Between O-frame and Encoder	C_4	1~10
	Between tube support and O-frame	C_5	2~20
	Between motor and flange	C_6	0.4~2
	Between U-frame1 and O-frame	C_7	5~20
	Between grazing incidence mirror mount and light entrance	C_8	5~30
	Between light entrance and filter	C_9	20~80
	Between box and box cover	C_{10}	1~10
	Between focal plane support and box cover	C_{11}	20~60
	Between focal plane substrate and thermal aluminum block	C_{12}	12~50
	Between CCD and thermal aluminum block	C_{13}	0.2~1.5
	Between thermal aluminum block and thermal strap	C_{14}	0.5~2.5
	Between CCD and focal plane substrate	C_{15}	30~100
	Between sunshade and tube1 of guide telescope	C_{16}	10~70
	Between tube1and tube 2 of guide telescope	C_{17}	2~15
	Between sunshade and filter of guide telescope	C_{18}	5~30
	Between front support and rear support of focal plane bracket	C_{19}	3~12
	Between box cover and radiant plate support	C_{20}	20~80
	Between control electric box and box	C_{21}	15~60
	Between CCD and adapter plate	C_{22}	3~15
	Between adapter plate and focal plane substrate	C_{23}	20~100
	Between motor 1 housing and flange	C_{24}	0.5~4
	Between motor 2 housing and flange	C_{25}	0.5~4
	Between motor and heat pipe	C_{26}	0.1~2
	Between box and side panel	C_{27}	0.5~3
	Between tube of guide telescope and tube support	C_{28}	5~20
	Between radiant plate support and radiant plate	C_{29}	20~60
	Between signal processing box and box cover	C_{30}	5~40
	Between radiant plate and thermal strap	C_{31}	0.2~2
	Between motor flange and O-frame	C_{32}	5~20
	Between focal plane substrate and back support	C_{33}	40~120
	Between tube of guide telescope and main tube support	C_{34}	2~10
	Between U-frame2 and O-frame	C_{35}	5~20
	Between signal processing box and side panel	C_{47}	0.2~1.5
	Between tube 1 and lens cover	C_{50}	10~40
Radiant heat transfer coefficient between MLI and components (W/m²/°C)	Between internal components and MLI	C_{36}	0.1~0.4
	Between lens cover and MLI	C_{37}	0.1~0.5
	Between turntable and MLI	C_{38}	0.1~0.5
	Between pedestal and MLI	C_{39}	0.1~0.5
	Between tube2 and MLI	C_{40}	0.1~0.5
	Between O-frame(-Z) and MLI	C_{41}	0.1~0.5
	Between O-frame(+Z) and MLI	C_{42}	0.1~0.5
	Between tube support and MLI	C_{43}	0.1~0.5
	Between guide telescope and MLI	C_{44}	0.1~0.5
	Between motor and MLI	C_{45}	0.1~0.5
	Between tube1 and MLI	C_{46}	0.1~0.5
Emissivity	Aluminum film surface	C_{48}	0.05~0.3
Thermal conductivity(W/m/K)	Copper thermal strap	C_{49}	150~400

5. Correction results and verification

After the above process of thermal analysis model correction, the work of the thermal analysis model correction is completed. The-low temperature condition is then used to verify the results. The temperature difference data of each TMP of pre- and post-corrections for the high-temperature and low-temperature conditions are listed in Table 4.

From Table 4 and Figures 8 and 9, based on the temperature data of the thermal balance test for the high-temperature condition, the maximum temperature difference after correction of the high-temperature condition has reduced from 11.5 °C to 1 °C, and the 70% temperature difference
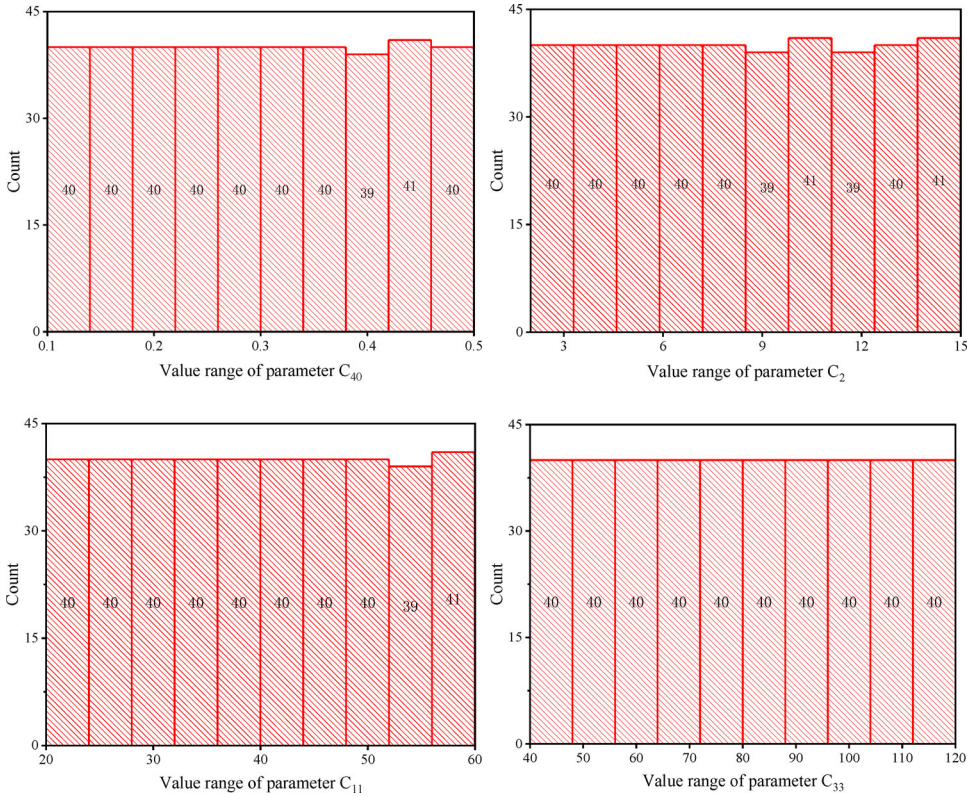
Figure 6. Frequency distribution histogram of four thermal design parameters.
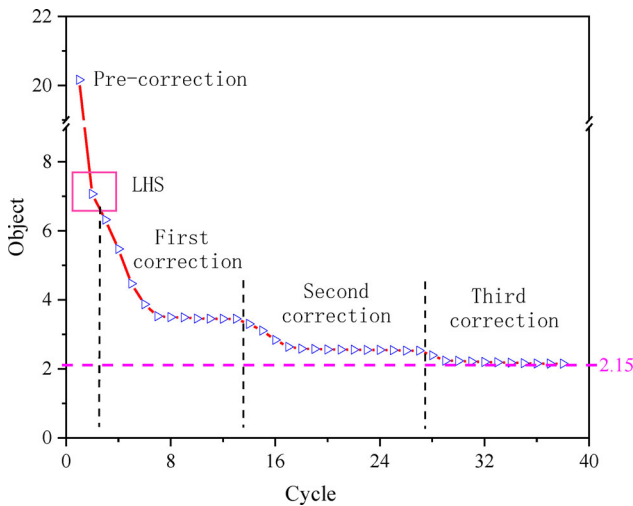

Figure 7. Objective function values in the process of correction.

is less than 0.5 °C. The maximum temperature difference after correction for the low-temperature condition is reduced from 11.5 °C to 1.95 °C, and the 75% temperature difference is less than 1.5 °C. The correction results show that the thermal analysis model correction method for which LHS and CRM are combined can effectively correct the thermal analysis model.
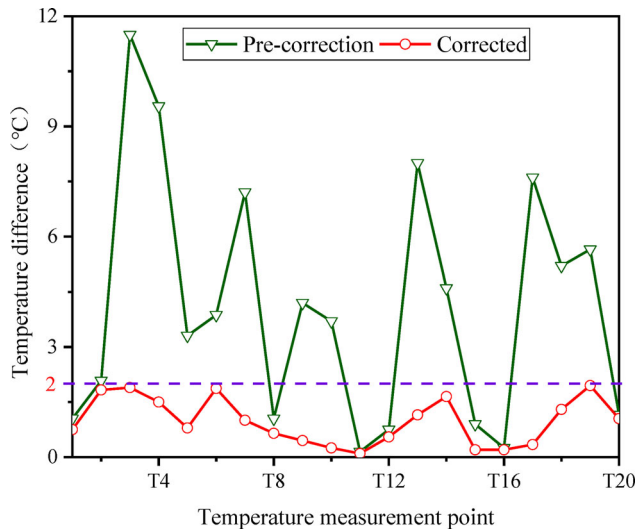
Table 4. Temperature difference of TMP of different conditions.

No.	TMP	Temperature difference at high temperature		Temperature difference at low temperature	
		Pre-correction	Corrected	Pre-correction	Corrected
1	T_1	1.15	1.00	1.05	0.75
2	T_2	0.54	0.09	2.08	1.83
3	T_3	11.50	0.90	11.50	1.90
4	T_4	10.00	0.10	9.55	1.50
5	T_5	4.30	0.10	3.31	0.79
6	T_6	2.55	0.65	3.87	1.87
7	T_7	0.55	0.05	7.21	1.01
8	T_8	0.65	0.60	1.05	0.65
9	T_9	2.20	0.05	4.20	0.45
10	T_{10}	6.90	0.05	3.70	0.25
11	T_{11}	0.45	0.45	0.15	0.10
12	T_{12}	1.35	0.45	0.75	0.55
13	T_{13}	5.85	0.20	8.00	1.15
14	T_{14}	1.40	0.05	4.60	1.65
15	T_{15}	1.10	0.65	0.90	0.20
16	T_{16}	0.60	0.45	0.25	0.20
17	T_{17}	6.15	0.00	7.61	0.34
18	T_{18}	3.80	0.00	5.20	1.30
19	T_{19}	1.00	0.90	5.65	1.95
20	T_{20}	1.25	0.35	1.15	1.05
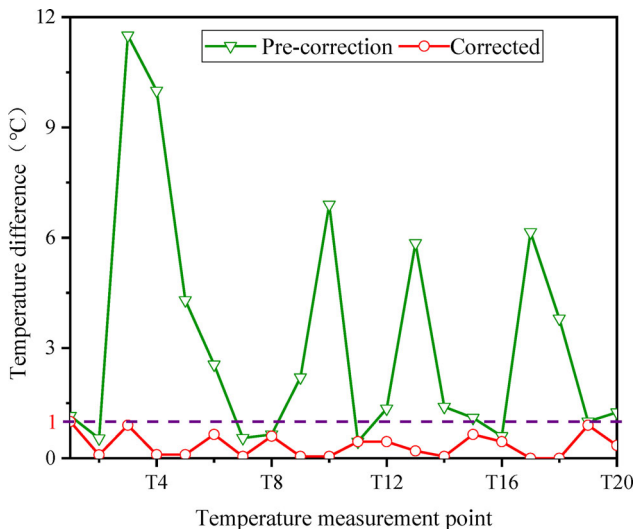
Figure 8. Temperature difference of TMP between pre-correction and corrected at high temperature.

6. Results and discussion

A thermal model correction method that combines LHS and CRM was proposed, and the idea of a layered correction is implemented in the process of correction. This method improves the correction efficiency, saves computation time, and reduces the blindness during corrections. This method is applied to the thermal analysis model corrections for the XEUVI, achieving improved results. After the correction, the maximum temperature difference of the TMP between the thermal simulation and the thermal balance test is less than $1\,°C$ for the high-temperature condition. Similarly, the maximum temperature difference is less than $2\,°C$ for the low-temperature condition. It turns out that this method can effectively correct the thermal analysis model, and thus

Figure 9. Temperature difference of TMP between pre-correction and corrected at low temperature.

provides a basis for establishing accurate models and a guarantee for predicting on-orbit temperatures of the spacecraft accurately.

Acknowledgments

Disclosure statement

The authors report there are no competing interests to declare in this article.

Funding

References

[1]   G. R. Min, *Satellite Thermal Control Technology*, 1st ed. Beijing: Aerospace Publishing House, 1991.

[2]   Z. Q. Hou, *Spacecraft Thermal Control Technology*. Beijing: China Science and Technology Press, 2007.

[3]   A. Robson, C. Heller, and H. Sdunnus, "Space systems thermal analysis software—a user's view," in International Conference on Environmental Systems and 8th European Symposium on Space Environmental Control Systems, 2005. DOI: 10.4271/2005-01-3052.

[4]   N. Liu, W. L. Cheng, and Q. Zhong, "Sensitivity analysis of spacecraft thermal model based on Mento-Carlo method," *Spacecraft Eng.*, vol. 18, no. 4, pp. 102–107, 2009.

[5]   V. Mareschi, V. Perotto, and A. Spazio, "Thermal test correlation with stochastic technique," in International Conference on Environmental Systems and 8th European Symposium on Space Environmental Control Systems, 2005. DOI: 10.4271/2005-01-2855.

[6]   J. Y. Zhang, H. P. Chang, and L. G. Wang, "Correction method for transient thermal analysis model of small satellite," *Chin. Space Sci. Technol.*, vol. 33, no. 4, pp. 24–30, 2013.

[7]   W. L. Cheng, N. Liu, and Q. Zhong, "Study on parameter correction method of steady-state thermal model for spacecraft," *J. Astronaut.*, vol. 31, no. 3, pp. 270–275, 2010.

[8]   S. J. Li, L. H. Chen, and Y. H. Wu, "Thermal design of detector for the solar x-ray and extreme ultraviolet imager," *J. Thermophys. Heat Transf.*, vol. 31, no. 2, pp. 1–7, 2018.

[9]   T. Beck, A. Bieler, and N. Thomas, "Numerical thermal mathematical model correlation to thermal balance test using adaptive particle swarm optimization (APSO)," *Appl. Therm. Eng.*, vol. 38, pp. 168–174, 2012. DOI: 10.1016/j.applthermaleng.2012.01.027.

[10]   H. N. Yang and Q. Zhong, "Monte-Carlo method for thermal model correction of spacecraft," *Spacecraft Eng.*, vol. 18, no. 3, pp. 53–58, 2009.

[11]   J. L. Deutsch and C. V. Deutsch, "Latin hypercube sampling with multidimensional uniformity," *J. Stat. Plan. Inference.*, vol. 142, no. 3, pp. 763–772, 2012. DOI: 10.1016/j.jspi.2011.09.016.

[12]   J. C. Helton and F. J. Davis, "Latin hypercube sampling and the propagation of uncertainty in analyses of complex systems," *Rel. Eng. System Saf.*, vol. 81, no. 1, pp. 23–69, 2003. DOI: 10.1016/S0951-8320(03)00058-9.

[13]   M. D. McKay, R. J. Beckman, and W. J. Conover, "A comparison of three methods for selecting values of input variables in the analysis of output from a computer code," *Technometrics.*, vol. 21, no. 2, pp. 239–245, 1979. DOI: 10.2307/1268522.

[14]   M. D. Mckay and R. J. Beckman, "Small sample sensitivity analysis techniques for computer-models, with an application to risk assessment – comments," *Commun. Stat. Theory Meth.*, vol. 9, no. 17, pp. 1859–1861, 1980. DOI: 10.1080/03610928008828000.

[15]   M. D. Shields and J. Zhang, "The generalization of Latin hypercube sampling," *Reliab. Eng. Syst. Saf.*, vol. 148, pp. 96–108, 2016. DOI: 10.1016/j.ress.2015.12.002.

[16]   S. M. Gong, *Applied Statistics*, 2nd ed. Beijing: Tsinghua University Press, 2005.

[17]   C. Q. Fan, "The amend method of the constrained coordinate supersede technic," *J. Hebei Univ. Sci. Technol.*, vol. 19, no. 2, pp. 74–78, 1998.

[18]   Z. Y. Wang, L. P. Sun, and Y. Yang, "Application of the coordinate alternation method to the numerical simulation of the temperature field in pistons," *Diesel Locom.*, vol. 384, no. 2, pp. 7–10, 2006.

[19]   C. Gong and Z. L. Wang, *Matlab Optimization Calculation*, 3rd ed. Beijing: Publishing House of Electronic Industry Press, 2014.